Yue-Jiao Zhang, Zhang-Fei Su[b], Jian-Feng Li[a,*], Jacek Lipkowski[b,*] What Vibrational Spectroscopy Tells about Water Structure at the Electrified Palladium-Water Interface, *J.Phys.Chen.C* , **2020**,*124*, 13240-13248

What Vibrational Spectroscopy Tells about Water Structure at the Electrified Palladium-Water Interface

Yue-Jiao Zhang[a], Zhang-Fei Su[b], Jian-Feng Li[a,], Jacek Lipkowski[b,*]*

[a]College of Energy, State Key Laboratory of Physical Chemistry of Solid Surfaces, iChEM, College of Chemistry and Chemical Engineering, Xiamen University, Xiamen 361005, China

[b]Department of Chemistry, University of Guelph, Guelph, Ontario N1G 2W1, Canada

KEYWORDS: ATR-SEIRAS, water structure, Palladium

ABSTRACT: The knowledge of structure and properties of water adsorbed on metal surfaces is relevant for understanding electrocatalytic reactions. A monolayer of Pd deposited at a gold electrode surface is known to have enhanced electrocatalytic properties. To shed new light on

these properties, the present study describes investigations of water structure at monolayer Pd film deposited at a nanostructured gold electrode consisting of ~50 nm large nanoparticles supported at a Si hemisphere. Attenuated Total Reflection Surface Enhanced Infrared Reflection Absorption Spectroscopy (ATR-SEIRAS) was applied to measure vibrational spectra of water molecules at the electrodes surface. The surface enhancement of the electric field of the photon allowed to determine spectra of water molecules interacting with Pd film. The results show that surface water is a mosaic of "ice-like", "liquid-like" and monomer or small clusters of water molecules. In addition, hydronium ions are present at the Pd surface in an acidic solution. The relative contribution of these structures depends on the pH and electrode potential. The surface water is more ordered at potentials corresponding to adsorption of hydrogen atoms.

1. INTRODUCTION

Pd metal finds many applications in heterogeneous catalysis.[1-3] The application of massive Pd in electrocatalysis is hindered by hydrogen absorption and Pd hydrides formation. This limitation is removed when a thin film of Pd is deposited on a gold surface. Several studies demonstrated that such electrodes display enhanced electrocatalytic activity towards formic acid oxidation,[4] glycerol oxidation,[5] hydrogen evolution[6, 7] and oxygen reduction.[8] Due to small (5%) mismatch between lattice constants of Au and Pd, thin films of Pd could form up to 4 monolayers (ML) thick pseudomorphic films at Au(111) single crystal electrodes.[9-13] Hydrogen absorption is not observed at films with 1 ML or 2 ML of Pd, but takes place at films with 3 and 4 ML of Pd. The electrode with 5 ML of Pd displays properties of massive Pd.[10-13] For the hydrogen evolution reaction, the enhanced electrocatalytic activity of Pd films and its dependence on film thickness

was correlated with an upward shift of the d-band center and an increase in the adsorption energy of hydrogen atom.[14, 15]

The reactions taking place at the metal-solution interface are also influenced by water adsorbed on metal surfaces. Therefore, detailed knowledge of the structure and properties of water molecules at the interfaces is an essential prerequisite to understand electrocatalytic reactions. The information concerning water at electrified interfaces is provided chiefly by surface enhanced infrared absorption spectroscopy studies introduced by Osawa's group.[16-19] At a nanopatterned electrode the molecules adsorbed at the metal surface experience two to three orders of magnitude enhanced electric field of the IR photon.[20, 21] Therefore absorption of IR photons by water molecules at the metal surface is much stronger than by molecules in the bulk. SEIRA was successfully used to study water structure at Au(111)[16, 17, 22-24] and Pt(111) surfaces.[19] Besides, Miyake et al.[25] reported SEIRA spectra of water on a film of Pd nanoparticles and Wandlowski and Pronkin[26] applied SEIRAS to study CO and sulfate adsorption at 1 ML Pd@Au electrode. However, they provided little information about the water structure at the Pd surface.

The objective of this study was to apply SEIRAS to describe the structure of water at a monolayer thick Pd film deposited at Au nanoparticles covered silicon surface (1ML Pd@Au). The film of Au nanoparticles was deposited using electroless method[27] improved by Cai's group[28, 29] for the deposition of other metals including Pd, Rh, Ru and Ni. Such film consists of Au nanoparticles with ~50 nm diameter preferentially oriented with (111) surface.[18, 27] The monolayer of Pd was deposited at Au nanoparticles by spontaneous irreversible replacement of a Cu adlayer.[30] This work shows that surface water is a mosaic of "liquid-like", "ice-like",

monomers and multimers (small clusters of water molecules) and hydronium ions in the acidic electrolyte. The populations of these structures depend on pH of the solution.

2. EXPERIMENTAL SECTION

2.1 Materials

HF (48%), NH_4F (>98%), NH_4Cl (≥99.5%), Na_2SO_3 (≥98%), $Na_2S_2O_3 \cdot 5H_2O$ (≥99.5%), $NaAuCl_4 \cdot 2H_2O$ (99%), $CuSO_4$ (≥99%) and Na_2PdCl_4 (98%) were obtained from from Sigma-Aldrich (Oakville, ON, CA). $NaClO_4$ (>99%) was purchased from Thermo Fisher Scientific (Whitby, ON, CA). All chemicals were used directly without further purification. All aqueous solutions were prepared using water from the Milli-Q (Millipore, Bedford, MA) ultrapure water system (resistivity > 18.2 MΩ cm).

2.2 Construction of the multiple layers of Pd on the nanostructured gold film on the silicon prism

The nanostructured gold film was deposited on a hemisphere silicon prism surface or silicon wafer surface by the electroless method developed in Osawa's group.[27] The silicon surface was immersed with 2% HF and then 40% NH_4F to remove the oxide layer and to terminate the surface with hydrogen. The deposition of the gold film was performed at 60 ^oC by adding a mixture of a plating solution (0.014 M $NaAuCl_4 \cdot 2H_2O$, 0.15 M Na_2SO_3, 0.05M $Na_2S_2O_3 \cdot 5H_2O$, and 0.05 M NH_4Cl) and 2% HF onto the hydrogen-terminated silicon surface. After deposition, the gold film covered silicon prism was stocked in water before use.

The 1 ML of Pd at the nanostructured gold film (1 ML Pd@Au) was prepared by the method of replacement of UPD of Cu.[30] The UPD of Cu was performed in 1 mM $CuSO_4$ + 0.1 M H_2SO_4 solution. A full monolayer Cu UPD on the Au electrode surface was obtained by controlling the

potentials at 0.0 V vs Ag/AgCl for two minutes. The monolayer Cu coated Au electrodes were then immediately immersed into 10 mM Na_2PdCl_4 solution for three minutes to completely replace Cu with Pd.

2.3 Electrochemical instrumentation and measurements

The electrochemical measurements were performed in an all-glass three-electrode cell. The nanostructured gold films on the silicon wafer surface were served as the working electrodes. The Ag/AgCl (saturated KCl) electrode (Pine Research Instrumentation, NC) was used as the reference electrode, and a gold coil was employed as the counter electrode. All potentials reported in this paper are quoted versus the Ag/AgCl (sat. KCl) electrode. Before each measurement, the cell was de-aerated by purging with argon (Praxair, Kitchener, ON, Canada) for 30 minutes. An argon blanket was maintained above the electrolyte throughout the experiments to prevent the influx of oxygen.

2.4 SEIRAS measurements

SEIRAS experiments were performed using a Thermo Nicolet Nexus 8700 spectrometer (Thermo Fisher Scientific, Mississauga, ON) with an all-glass three-electrode cell. The silicon prism covered with Pd monolayers (1 ML Pd@Au) was served as the working electrode.

The SEIRA measures differential spectra defined as:

$$\Delta A = \log(\frac{I_0}{I}) \tag{1}$$

where I and I_0 are the reflections measured at the sample potential E and the reference potential which was equal to +0.3 V vs Ag/AgCl in 0.1 M $NaClO_4$ solution and +0.6 V vs Ag/AgCl in 0.1 M $HClO_4$ solution; ($\Delta A = A(E) - A(+0.3V)$ in neutral solution and $\Delta A = A(E) - A(+0.6)$ in acidic solution), where $A(E)$ is the absorbance at the sample potential E and $A(+0.3V)$ or $A(+0.6V)$ is the absorbance at the reference electrode potential. The sample spectra were collected for

potentials *E* from +0.3 V to -0.8 V vs Ag/AgCl in neutral solution and from +0.5V to -0.2V vs Ag/AgCl in the acidic solution with 0.1 V interval. At each potential, 500 IR scans were added and averaged with the instrumental resolution of 4 cm^{-1}.

3. RESULTS AND DISCUSSION

3.1 Electrochemical characterization

Figure 1 shows a typical cyclic voltammogram (CV) recorded for 1 ML Pd@Au electrode in (i) 0.1 M $NaClO_4$ (red curve) and (ii) 0.1 M $HClO_4$ at a scan rate of 50 mV s^{-1}. The curves are shifted along the potential axis by ~0.36 V as expected for the difference between the onset of hydrogen evolution reaction in the two electrolytes. The hydrogen adsorption region is between -0.2 and -0.6 V vs Ag/AgCl in 0.1 M $NaClO_4$ and between 0.05 and -0.2V vs Ag/AgCl in 0.1 M $HClO_4$ solution. The onset of Pd oxidation is ~0.2 V vs Ag/AgCl in the neutral and at ~0.6 V vs Ag/AgCl in the acidic solution. The small peak at $E > 0.2$ V observed on the positive-going scan is ascribed to the oxidation of the Pd surface, and the peak at 0.0 V on the reverse negative-going sweep is due to the reduction of surface oxide.

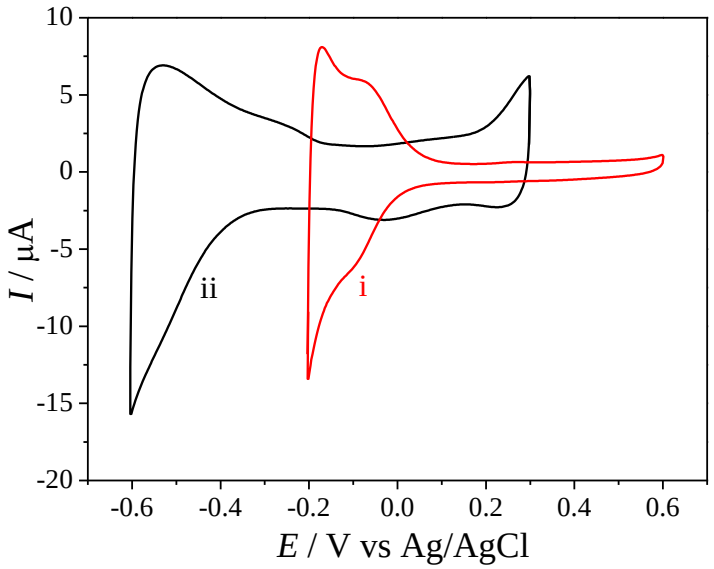

Figure 1. Cyclic voltammogram for the 1 ML Pd@Au electrode in (i) 0.1 M $NaClO_4$ (black curve) and (ii) 0.1 M $HClO_4$ (red curve) recorded at 50 mV s^{-1}.

To identify this feature surface enhanced Raman spectroscopy (SERS) was performed using the 1 ML Pd@Au electrode. The SERS spectra are presented in Figures S1 (A) and (B) of the Supporting information. They show that by moving potential in a positive direction the onset of Pd oxide formation takes place at E > 0.4 V vs Ag/AgCl.[31, 32] On the reverse scan, the oxide disappears at E <-0.1 V vs Ag/AgCl in a good agreement with the shape of CV. The hydrogen adsorption and oxide formation are separated by about ~0.4 V long double layer regions. Differential capacitance curves, shown in Figure S2(A) of the supporting information, were measured for several concentrations of the two electrolytes to determine the value of the capacitance and the potential of zero charge. For the neutral electrolyte, the curve recorded for 0.01 M $NaClO_4$ displays a diffuse layer minimum at E=-0.11 V vs Ag/AgCl indicating the position of the potential of zero charge (E_{pzc}). This result agrees well with earlier measurement by El-Aziz et al.[33] Figure S2(B) shows that the diffuse layer minimum is absent in the diluted solution of $HClO_4$. For 0.01 M $HClO_4$ solution, Alvarez et al.[34] determined the potential of zero total charge at Pd islands covering Au(111) surface to be equal to 0.25 V vs RHE which corresponds to -0.125 V vs Ag/AgCl electrode. This number is in excellent agreement with E_{pzc} determined above for 0.1 M $NaClO_4$ solution. The CVs in Figure 1 demonstrates that hydrogen adsorption takes place at potentials close to E_{pzc} in acidic solutions. Besides, the capacitance in the double layer region is ~5 times smaller in the acidic electrolytes causing difficulties to detect the diffuse layer minimum. The differences in the double layer capacitance suggest significant differences in the surface water structure discussed below.

3.2 SEIRAS studies in 0.1 M $NaClO_4$ solution

The SEIRA spectra of water at the 1 ML Pd@Au electrode are shown in Figure 2. The spectra were collected with -0.1 V intervals within the potential range between +0.2 V and -0.8 V vs Ag/AgCl. Each spectrum represents the difference in absorbance at the specified potential and the reference potential of +0.3 V vs Ag/AgCl. Figure 2 shows pronounced potential-induced changes corresponding to the O-H stretching (ν(OH)) of water between 3000 and 3800 cm^{-1} and the H-O-H bending vibrations (δ(HOH)) around 1640 cm^{-1}. The small bands at ~2300 cm^{-1} are due to residual CO_2 in the gas phase. The intensity of water bands increases within the potential range from +0.2 V to -0.8 V vs Ag/AgCl.

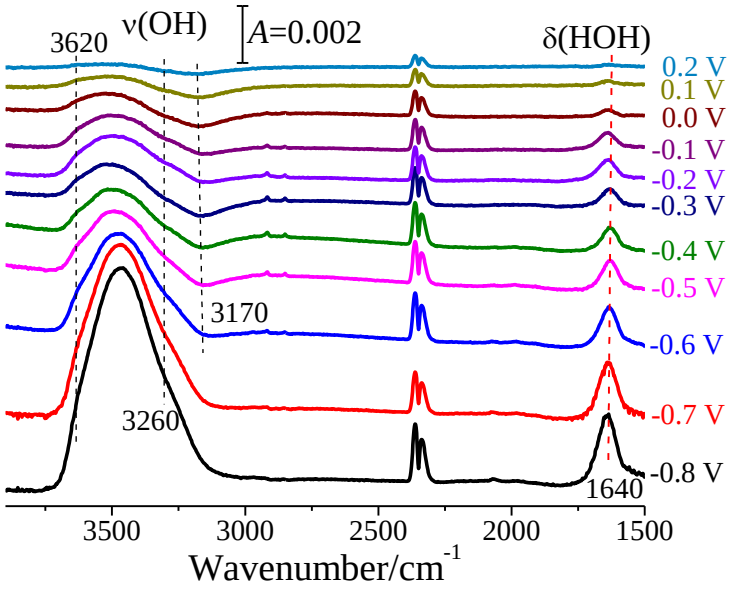

Figure 2. Potential difference spectra of water at the 1 ML Pd@Au electrode in 0.1 M $NaClO_4$ calculated by using the spectrum at 0.3 V as the reference.

Figure 3 plots the normalized ν(OH) and δ(HOH) bands with comparable intensities at all potentials, to reveal changes in their shape. The ATR spectra of water, recorded using the silicon window, are also plotted on the top of these figures. The ATR spectrum represents absorption by

water molecules of an evanescent wave penetrating hundreds of nanometers into the bulk and hence represents the spectrum of bulk water.

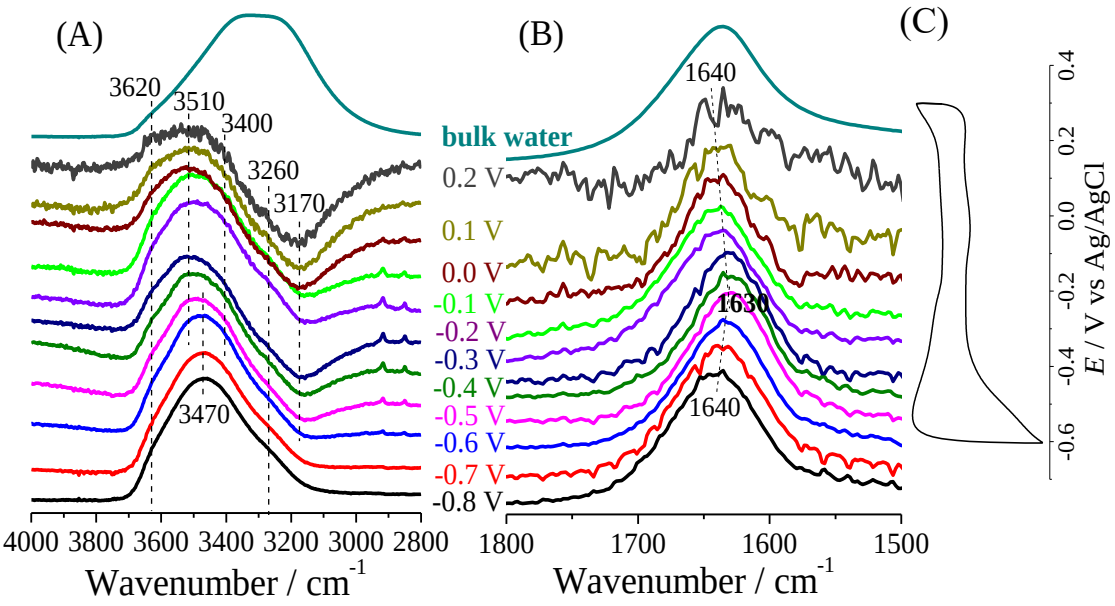

Figure 3. Normalized of (A) νOH and (B) δ(HOH) bands in 0.1 M $NaClO_4$. The SEIRA spectra are aligned with potentials corresponding to the CV curve (C).

The CV plotted in Figure 3(C) demonstrates that the negative band around 3170 cm^{-1} disappears at potentials corresponding to hydrogen adsorption. In contrast to the ν(OH) bands, the δ(HOH) bands are always positive demonstrating that the bending band intensity is always stronger at the sample potential than at the reference potential. The shape of bending bands in SEIRA spectra is similar to the shape of this band in the ATR spectrum.

To estimate the contribution of water in the first layer interacting with Pd to the SEIRA spectra, a spectrum for the electrode covered by a monolayer of CO was recorded. The monolayer of CO displaces the first layer of water molecules from the Pd surface and the spectrum recorded at that electrode corresponds to water molecules present on top of CO and in

more distant layers. Figure S3 of SI compares spectra recorded at 1 ML Pd@Au electrode with and without CO, at *E*=-0.6 V vs Ag/AgCl. The spectrum of water at CO covered is about an order of magnitude smaller than the spectrum recorded at CO free surface. This indicates that water molecules interacting with Pd contribute to about 90% of the total intensity of spectra measured at the clean surface.

The broad band envelope of the ν(OH) region contains several sub-bands. The Fourier self-deconvolution (FSD) procedure was employed to resolve the fine band structure in this region. The FSD narrows the IR bands and reveals the presence of sub-bands in a broad spectral envelope.[35] The FSD of the ATR spectrum of bulk water and selected SEIRAS bands are plotted in Figure 4. The FSD of the ATR spectrum reveals that the ν(OH) band of bulk water could be decomposed into three sub-bands at ~3220, ~3390 and 3610 cm^{-1}. The bands at 3220 and 3390 cm^{-1} correspond to water molecules in a network of hydrogen bonds (network water). The band at 3220 cm^{-1} is referred to as "ice-like water band" and corresponds to in-phase OH stretching coupled to Fermi overtones of bending vibration. The band at 3390 cm^{-1} is called "liquid-like water band" and corresponds to stretching vibrations of water molecules forming a network of weaker hydrogen bonds. The band at 3610 cm^{-1} corresponds to water molecules with a disturbed network of hydrogen bonds (monomer or multimer water molecules).[36-40]

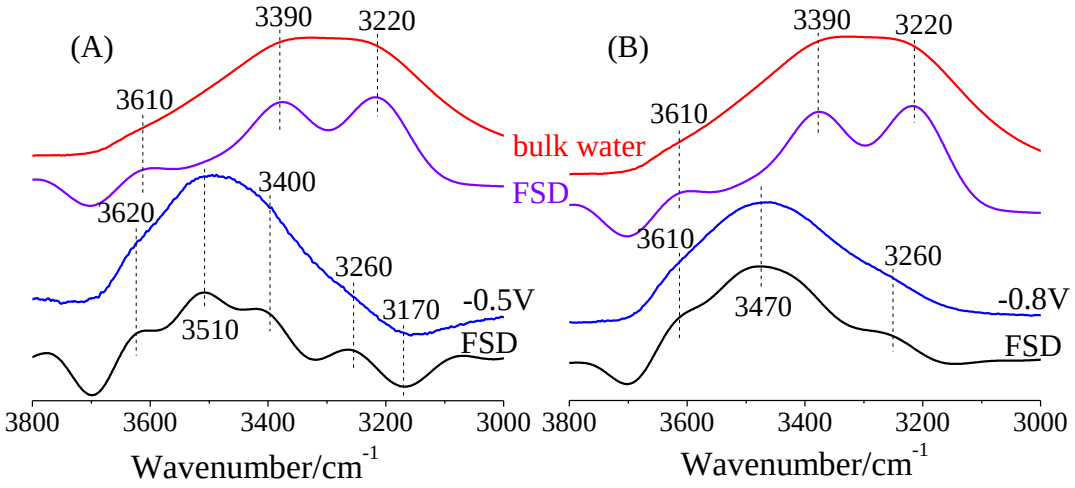

Figure 4. FSD of SEIRA spectra of the water at the 1ML Pd@Au at (A) -0.5 V and (B) -0.8 V vs Ag/AgCl. The top red curve is the ATR spectrum of bulk water. The dashed lines plot the FSD result of the ATR spectrum.

The SEIRA spectra of water at the 1 ML Pd@Au are significantly shifted to higher wavenumbers. Besides, the negative band at ~3170 cm^{-1} has a positive counterpart at 3260 cm^{-1}. The appearance of bipolar features in the region of "ice-like water" indicates that the "ice-like water" band is stronger at *E*=+0.3V vs Ag/AgCl than at more negative potentials. Bands at higher wavenumbers are positive indicating that they are more intense than the corresponding bands at *E*=+0.3V vs Ag/AgCl. The FSD reveals that the IR spectra of the water at the 1 ML Pd@Au at -0.5 V (Figure 4(A)) has additional bands at ~3400 and 3510 cm^{-1} corresponding to "liquid-like water" with progressively weaker hydrogen bonds network and a band at ~3620 cm^{-1} corresponding to multimer or monomer water molecules. Hydrogen bonds between water molecules cause a weakening of the covalent water O-H bond, leading to the decrease of the ν(OH) frequency. The position and intensity of the ν(OH) band provide valuable information regarding the structure of the interfacial water. The FSD spectra in Figure 4 show that all three

forms of water are present at the Pd surface. However, the “liquid-like water” bands in SEIRAS spectra are blue shifted relative to the position of these bands in the spectrum of bulk water and hence have weaker hydrogen bonds network.

Figures 5A plots positions of global maximum for the ν(OH) and δ(HOH) bands as a function of the electrode potential. The data are presented up to -0.1 V vs Ag/AgCl. At more positive potentials the pronounced negative lob of the band at the reference potential is distorting the shape and position of the global maximum of the ν(OH) band. In addition, SERS spectra (Figure S1 of SI) showed that PdO could be formed at these potentials. The band positions change in opposite directions for the two bands. This is typical behavior. Hydrogen bonding is known to decrease the O-H stretching frequency and to increase the H-O-H bending frequency. Bending and stretching frequencies of water anti-correlate.[41] The plot for ν(OH) displays a maximum and the plot for δ(HOH) a minimum at ~-0.3 V vs Ag/AgCl. In the double layer region (from -0.1 to -0.3 V vs Ag/AgCl) the frequency of ν(OH) band increases and consistently the position of the δ(HOH) decreases when potential moves in the negative direction. The onset of hydrogen adsorption changes this trend. The decrease of ν(OH) and the increase of δ(HOH) frequencies indicates that hydrogen adsorption strengthens the formation of a hydrogen bond network. Figure S4 of SI shows the dependence of the band intensities of the stretching and bending bands on the electrode potential. After an initial increase at positive potentials, the intensity plots show a quasi-plateau with a shallow minimum at E=-0.3V vs Ag/AgCl. It correlates well with the maximum on the ν(OH) and minimum of the δ(HOH) plots in Figure 5(A). A change of the band intensity may be caused by either a change in the orientation or a change in the density of surface water. The presence of the minimum suggests that it is caused by a reorientation of water

molecules. Figure S4 shows that the band intensities significantly increase at the potentials of hydrogen adsorption.

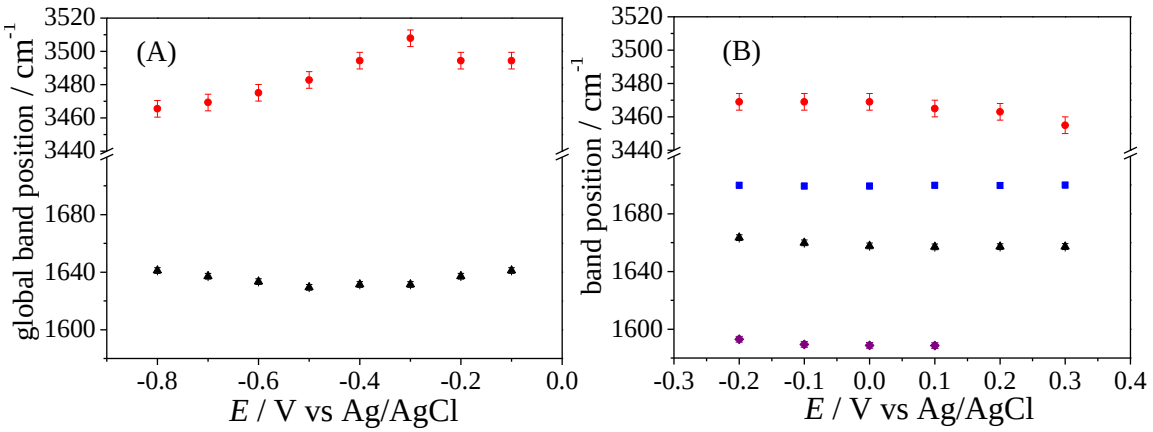

Figure 5. (A) Variation of the global band maximum position of the water ν(OH) (red circles) and δ(HOH) (black circles) bands in 0.1 M $NaClO_4$. (B) Variation of the global band maximum position of the water ν(OH) (red circles) and δ(HOH) of hydronium ion at 1700 cm^{-1} (blue rectangles), δ(HOH) of network water at 1660 cm^{-1} (black circles) and δ(OH) of water monomer at 1590 cm^{-1} (purple diamonds) in 0.1 M $HClO_4$.

The ratio of absorbance at 3610 cm^{-1} (A_{3610}) to absorbance at 3400 cm^{-1} (A_{3400}):[38, 40, 42]

$$R_{\text{multimer}} = \frac{A_{3610}}{A_{3400}} \qquad (2)$$

could be used to estimate the population of monomers or multimers of water molecules. Figure 6 displays changes in R_{multimer} as a function of the applied potential. R_{multimer} calculated from the ATR spectrum for bulk water is equal to 0.17. Figure 6 shows that at the potentials of hydrogen adsorption the values of R_{multimer} are comparable to the value observed for bulk water. The values of R_{multimer} decrease at E>-0.5V vs Ag/AgCl, indicating that the population of monomers and multimers is smaller in the double layer region. Overall, the SEIRA spectra recorded in neutral

solutions at 1 ML Pd@Au demonstrate that the surface has predominantly "liquid-like water" properties with a small population of monomers and multimers. The "liquid-like water" band position is blue shifted relative to the same band in bulk water indicating that the hydrogen bonds network of water at the Pd@Au surface is weakened. Hydrogen adsorption causes a small strengthening of the hydrogen bonds network and a small increase in the population of monomers and multimers of water molecules. However, both stretching and bending bands intensities significantly increase in this region indicating that adsorbed hydrogen has a strong impact on the orientation or a change in the density of surface water.

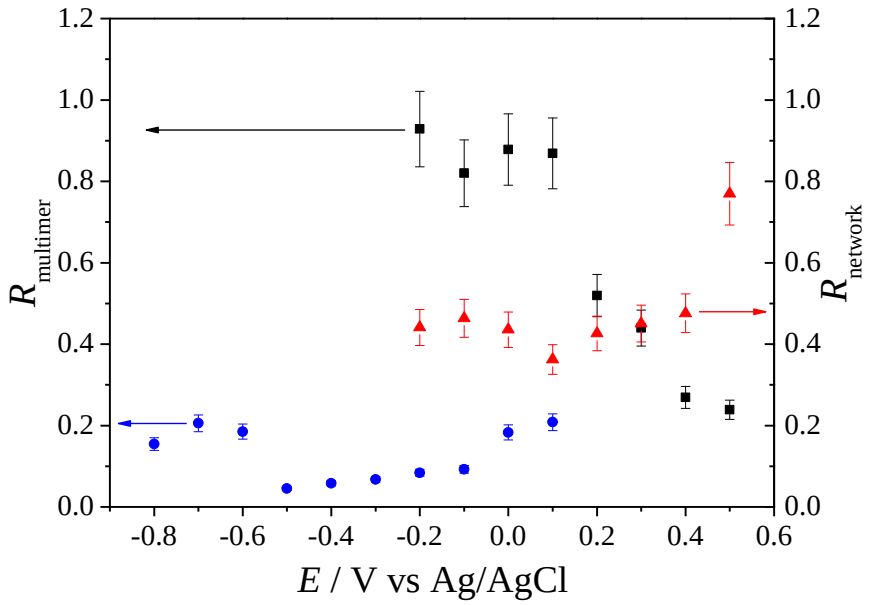

Figure 6. Left y-axis: variation of $R_{multimer}$ in 0.1 M $NaClO_4$ (blue circles) and 0.1 M $HClO_4$ (black squares) as a function of applied potential. Right y-axis: Variation of $R_{network}$ in 0.1 M $HClO_4$ (red triangles).

3.3 SEIRAS studies in 0.1M $HClO_4$ solution

Figure 7(A) shows the ν(OH) region of the SEIRAS spectra recorded at the 1 ML Pd@Au electrode in 0.1 M $HClO_4$ solution. The spectra were collected with -0.1 V intervals within the potentials range between +0.5 V and -0.2 V vs Ag/AgCl. Each spectrum represents the difference between absorbance at the specified potential and the reference potential of +0.6 V vs Ag/AgCl. In the acidic solution, the SEIRA spectra are always positive indicating that the intensity of water bands at the reference potential is weaker than at more negative potentials. This behavior is different from that observed in 0.1 M $NaClO_4$ solution. It suggests that in the neutral solution, the strong negative lob in the region of "ice water" (Figure 3) may be caused by the presence of PdO at the reference potential, templating the "ice water" structure. In 0.1 M $HClO_4$ solution, the PdO is absent. Figure 7(B) plots the normalized spectra. They facilitate observation of changes in band shapes with potential. The band at most positive potential +0.5V vs Ag/AgCl is similar in shape to the band of bulk water. However, bands at more negative potentials are significantly shifted to higher wavenumbers, indicating a weakening of hydrogen bonds network.

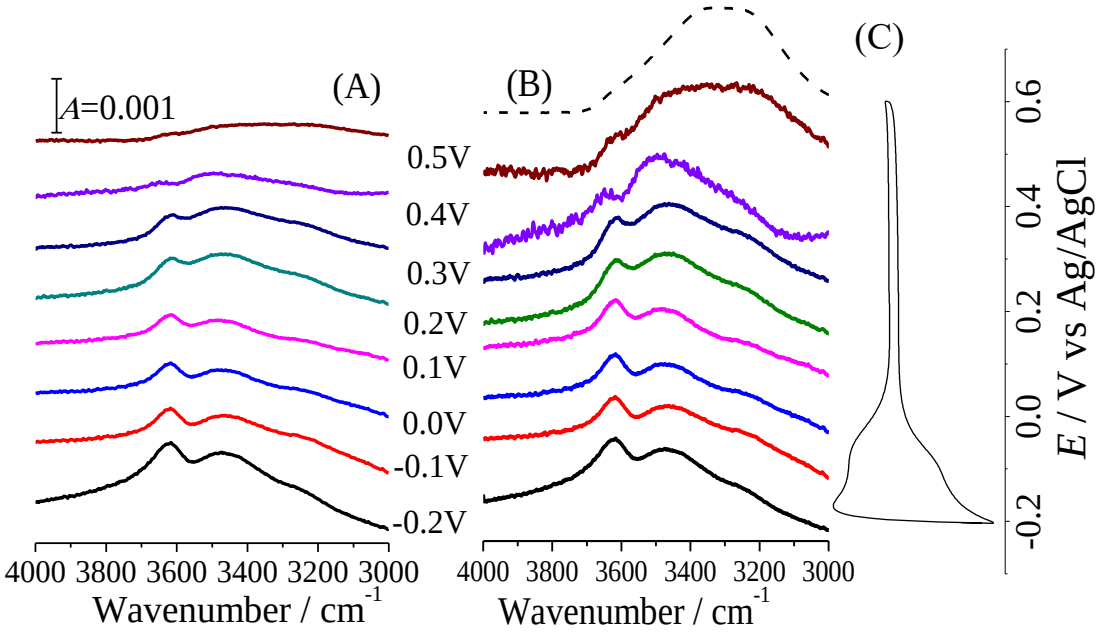

Figure 7. Potential difference SEIRA spectra (A) and normalized SEIRA spectra (B) in the ν(OH) region of water at the 1 ML Pd@Au in 0.1 M $HClO_4$. The spectra are aligned with potentials corresponding to the CV curve (C). The dashed line in Figure 7(B) plots the ATR spectrum of bulk water.

Their broad band envelope contains several sub-bands. The FSD procedure was employed to resolve the fine band structure. The FSD of a selected potential is plotted in Figure 8(A). The FSD for additional potentials is shown in Figure S5 of SI. The FSD reveals that SEIRA spectra contain three sub-bands assigned to: "multimer water" (at ~3620 cm^{-1}), "liquid-like water" (at ~3470 cm^{-1}) and "ice-like water" (at ~3240 cm^{-1}) at all potentials. The position of "ice-like water" bands in the SEIRA spectra and in the ATR spectrum of bulk water are similar. In contrast, the "liquid-like water" bands are shifted to higher wavenumbers in SEIRAS spectra, indicating a weakened network of hydrogen bonds. Figure 5(B) shows that its frequency is equal to 3470 cm^{-1} at negative potentials and decreases to 3460 cm^{-1} at positive end of potentials. In the acidic solution, wavenumbers of this band are somewhat lower than in the neutral solution, suggesting a somewhat stronger network of hydrogen bonds. Figure S6(A) of SI plots intensities of the "liquid-like water" band at ~3470 cm^{-1} and the "multimer" band at ~3620 cm^{-1} as a function of the electrode potential. The intensity of the "liquid-like" band displays a minimum at ~0.1 V vs Ag/AgCl. The "multimer" band increases monotonically with more negative potentials. At potentials of hydrogen adsorption (E<0.0 V vs Ag/AgCl) the two bands have comparable magnitude and increase sharply indicating that hydrogen adsorption has a strong impact on the orientation or an increase of surface water density, in analogy to the behavior observed earlier in the neutral solution.

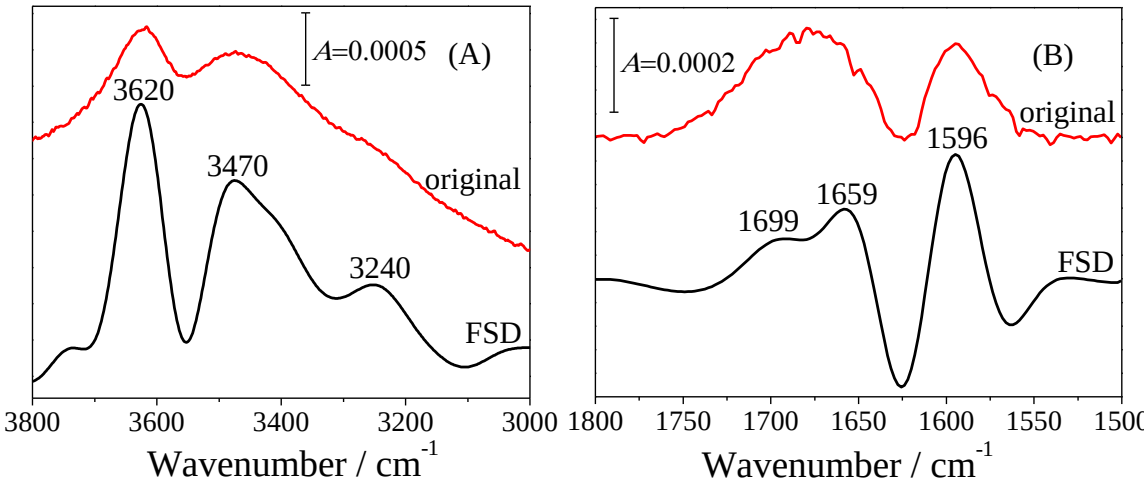

Figure 8. SEIRA spectra (red) and FSD results (black) of water at the 1 ML Pd@Au in 0.1 M $HClO_4$ at E=-0.2 V. (A) ν(OH) and (B) δ(HOH) region.

The structure of water can be further quantified by calculating $R_{network}$ defined as a ratio of absorbance at 3240 cm^{-1} (A_{3240}) to absorbance at 3470 cm^{-1} (A_{3470}).[38, 40, 42] For comparison with the neutral solution, the values of $R_{network}$ are plotted in Figure 6. They are approximately equal to 0.4 and display a shallow minimum at E=+0.1 V vs Ag/AgCl corresponding to the minimum observed on the band intensity plot in Figure S6(A). The $R_{network}$ calculated from the ATR spectrum of bulk water is equal to 0.67. These numbers indicate that water at the Pd@Au surface has less "ice-like water" than in the bulk and that the "liquid-like water" is the predominant structure. The band corresponding to "multimer" water is strong in the acidic solution and is blue shifted relative to the bulk water. The values of $R_{multimer}$ are also plotted in Figure 6 as a function of electrode potential. They are about an order of magnitude higher than in the neutral solution. A comparison with CV (Figure 7(C)) shows that $R_{multimer}$ is particularly high at potentials corresponding to hydrogen adsorption. Its values progressively diminish when potential becomes

more positive. At all potentials, $R_{multimer}$ is higher than the value 0.17 in bulk water, indicating that in acidic solutions surface water has a high population of monomers and/or multimers.

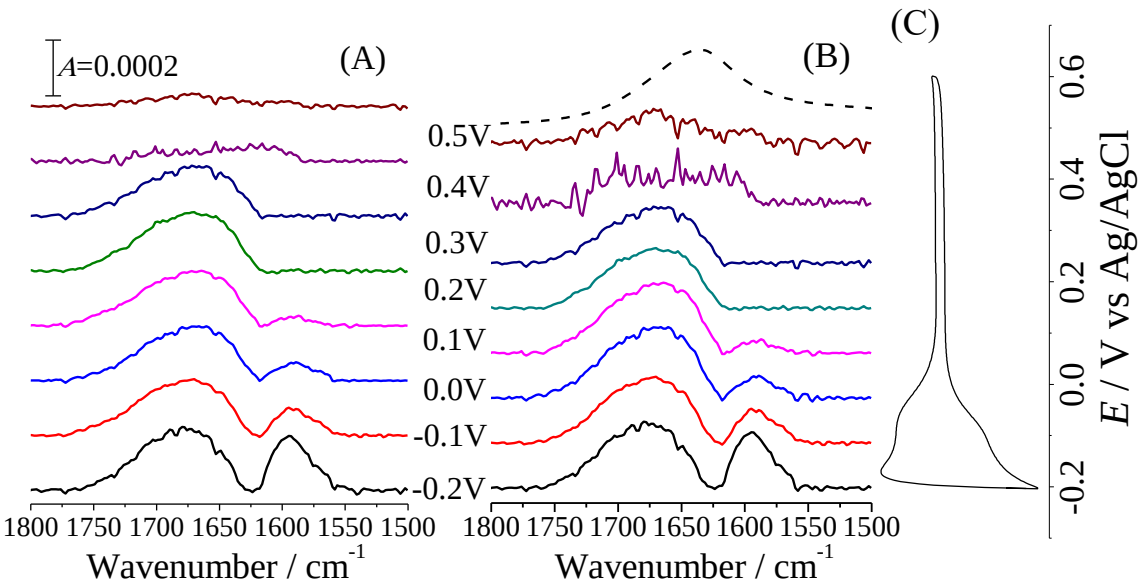

Figure 9. Potential difference SEIRA spectra (A) and normalized SEIRA spectra (B) of δ(HOH) of water at the 1 ML Pd@Au in 0.1 M $HClO_4$. (C) The spectra are aligned with potentials corresponding to the CV curve. The dashed line in Figure 9(B) plots the ATR spectrum of bulk water.

The IR spectra in the δ(HOH) region provide further information about the properties of surface water. Figure 9(A) shows measured and Figure 9(B) plots normalized SEIRA spectra in this region. In 0.1 M $HClO_4$ solution, the δ(HOH) bands are different than spectra recorded in 0.1 M $NaClO_4$ and for bulk water. They display two bands; one at ~1675 cm^{-1} and a second at more negative potentials at ~ 1600 cm^{-1}. The FSD analysis in Figure 8(B) shows that the broad band at ~1670 cm^{-1} consists of two sub-bands centered at ~1700 and ~ 1660 cm^{-1}. The band at ~1700 cm^{-1} has been observed by Osawa et al.[19] at Pt(111) and Garcia-Araez et al.[23] at Au(111)

in $HClO_4$ solutions and was assigned to hydronium ion based on UHV studies by Wagner and Moylan[43] and Chen et al.[44] The band at ~1590 cm^{-1} has been assigned to "monomer" water. Indeed, the changes of its intensity correlate well with changes of the stretching band at ~ 3620 cm^{-1}. The band at 1660 cm^{-1} is assigned to network water. Figure S6(B) of SI plots intensities of the three bands as a function of the electrode potential. The bands corresponding to hydronium ion and network water have a comparable intensity and display a shallow minimum at ~0.1 V vs Ag/AgCl, similar to the minimum displayed by the ν(OH) band of "network water" in Figure S6(A) of SI. In contrast, the band of "monomer water" is observed at E<0.1V vs Ag/AgCl and increases fast in the region of hydrogen adsorption.

There are significant differences between the properties of water at the 1 ML Pd@Au in acidic and neutral solutions. The band of hydronium ion is present in the IR spectra recorded in the acidic solution. Its intensity increases when the potential becomes more negative. The band corresponding to "monomer/multimer" water is weak in neutral solutions and strong in acidic solution. The IR spectra recorded in the two solutions have strong bands of "liquid-like water" which indicates that large fractions of surface water form disturbed network of hydrogen bonds. This network is somewhat more disturbed in acidic solution.

4. CONCLUSIONS

At monolayer Pd/@Au electrodes the surface water consists of a mosaic of 'ice-like water", "liquid-like water", monomers or multimers and hydronium ions. The relative population of these structures depends on pH and hydrogen atom adsorption. In the neutral solution, "liquid water" is the predominant structure. However, it is less ordered than water in the bulk. The population of "monomers" or small clusters of water molecules is very low and hydronium ions

are absent. The surface water is more ordered in acidic solutions. The band of "ice-like water" is quite strong, however, the population of "ice-like water" is lower than in the bulk. The "liquid-like" water predominates. It is less ordered than in the bulk water but more ordered than surface water in the neutral electrolyte. A new feature in acidic solution is a strong presence of hydronium ions and a visible population of "monomers" or small clusters of water molecules.

ASSOCIATED CONTENT

Supporting Information.

The Supporting Information is available free of charge on the ACS Publications website.

SERS spectra of the 1 ML Pd@Au electrode in 0.1 M $NaClO_4$, differential capacitance curves recorded for the 1 ML Pd@Au electrode in different solutions, SEIRAS spectra of the 1 ML Pd@Au with and without CO, variation of the global maxima of the ν(OH) stretching and δ(HOH) bending band, SEIRA spectra and FSD results at different potentials in 0.1 M $HClO_4$.(PDF)

AUTHOR INFORMATION

Corresponding Author

* E-mail: li@xmu.edu.cn

* E-mail: jlipkows@uoguelph.ca

Author Contributions

The manuscript was written through contributions of all authors. All authors have given approval to the final version of the manuscript.

ACKNOWLEDGMENT

This work was supported by a grant from Natural Sciences and Engineering Research Council of Canada (NSERC) to JL (RG-03958), National Natural Science Foundation of China (NSFC) (21925404 and 21775127), "111" Project (B17027), and National Key Research and Development Program of China (2019YFA0705400 and 2019YFD0901100).

REFERENCES

(1) Plauck, A.; Stangland, E. E.; Dumesic, J. A.; Mavrikakis, M. Active sites and mechanisms for H_2O_2 decomposition over Pd catalysts. *Proc. Natl. Acad. Sci. U.S.A.* **2016,** *113*, E1973-E1982.

(2) Duss, M.; Vallooran, J. J.; Salvati Manni, L.; Kieliger, N.; Handschin, S.; Mezzenga, R.; Jessen, H. J.; Landau, E. M. Lipidic Mesophase-Embedded Palladium Nanoparticles: Synthesis and Tunable Catalysts in Suzuki–Miyaura Cross-Coupling Reactions. *Langmuir* **2018,** *35*, 120-127.

(3) Chen, Z.; Liu, Y.; Liu, C.; Zhang, J.; Chen, Y.; Hu, W.; Deng, Y. Engineering the Metal/Oxide Interface of Pd Nanowire@ CuOx Electrocatalysts for Efficient Alcohol Oxidation Reaction. *Small* **2019**, 1904964.

(4) Baldauf, M.; Kolb, D. Formic acid oxidation on ultrathin Pd films on Au (hkl) and Pt (hkl) electrodes. *J. Phys. Chem.* **1996,** *100*, 11375-11381.

(5) Mello, G. A.; Busó-Rogero, C.; Herrero, E.; Feliu, J. M. Glycerol electrooxidation on Pd modified Au surfaces in alkaline media: Effect of the deposition method. *J. Chem. Phys.* **2019,** *150*, 041703.

(6) Kibler, L. Dependence of electrocatalytic activity on film thickness for the hydrogen evolution reaction of Pd overlayers on Au (1 1 1). *Electrochim. Acta* **2008,** *53*, 6824-6828.

(7) Schäfer, P. J.; Kibler, L. A. Incorporation of Pd into Au (111): enhanced electrocatalytic activity for the hydrogen evolution reaction. *Phys. Chem. Chem. Phys.* **2010,** *12*, 15225-15230.

(8) Naohara, H.; Ye, S.; Uosaki, K. Electrocatalytic reactivity for oxygen reduction at epitaxially grown Pd thin layers of various thickness on Au (111) and Au (100). *Electrochim. Acta* **2000,** *45*, 3305-3309.

(9) Takahasi, M.; Hayashi, Y.; Mizuki, J.-I.; Tamura, K.; Kondo, T.; Naohara, H.; Uosaki, K. Pseudomorphic growth of Pd monolayer on Au (111) electrode surface. *Surf. Sci.* **2000,** *461*, 213-218.

(10) Baldauf, M.; Kolb, D. A hydrogen adsorption and absorption study with ultrathin Pd overlayers on Au (111) and Au (100). *Electrochim. Acta* **1993,** *38*, 2145-2153.

(11) Kibler, L.; Kleinert, M.; Randler, R.; Kolb, D. Initial stages of Pd deposition on Au (hkl) Part I: Pd on Au (111). *Surf. Sci.* **1999,** *443*, 19-30.

(12) Kibler, L.; El-Aziz, A.; Kolb, D. Electrochemical behaviour of pseudomorphic overlayers: Pd on Au (1 1 1). *J. Mol. Catal. A-Chem* **2003,** *199*, 57-63.

(13) Tang, J.; Petri, M.; Kibler, L.; Kolb, D. Pd deposition onto Au (111) electrodes from sulphuric acid solution. *Electrochim. Acta* **2005,** *51*, 125-132.

(14) Roudgar, A.; Groß, A. Local reactivity of thin Pd overlayers on Au single crystals. *J. Electroanal. Chem.* **2003,** *548*, 121-130.

(15) Roudgar, A.; Groß, A. Local reactivity of metal overlayers: Density functional theory calculations of Pd on Au. *Phys. Rev. B* **2003,** *67*, 033409.

(16) Osawa, M.; Ataka, K.-i.; Yoshii, K.; Yotsuyanagi, T. Surface-enhanced infrared ATR spectroscopy for in situ studies of electrode/electrolyte interfaces. *J. Electron. Spectrosc.* **1993,** *64*, 371-379.

(17) Ataka, K.; Yotsuyanagi, T.; Osawa, M. Potential-dependent reorientation of water molecules at an electrode/electrolyte interface studied by surface-enhanced infrared absorption spectroscopy. *J. Phys. Chem.* **1996,** *100*, 10664-10672.

(18) Osawa, M. In-situ surface-enhanced infrared spectroscopy of the electrode/solution interface. In *Advances in Electrochemical Science and Engineering*, Alkire, R.; Kolb, D. M.; Lipkowski, J.; Ross, P. N., Eds.; Weinheim: Germany, 2006; Vol. 9, pp 269-313.

(19) Osawa, M.; Tsushima, M.; Mogami, H.; Samjeske, G.; Yamakata, A. Structure of water at the electrified platinum− water interface: A study by surface-enhanced infrared absorption spectroscopy. *J. Phys. Chem. C* **2008,** *112*, 4248-4256.

(20) Osawa, M. Dynamic processes in electrochemical reactions studied by surface-enhanced infrared absorption spectroscopy (SEIRAS). *Bull. Chem. Soc. Jpn* **1997,** *70*, 2861-2880.

(21) Osawa, M. Surface-enhanced infrared absorption. In *Near-field optics and surface plasmon polaritons*; Springer, 2001, pp 163-187.

(22) Wandlowski, T.; Ataka, K.; Pronkin, S.; Diesing, D. Surface enhanced infrared spectroscopy—Au (1 1 1-20 nm)/sulphuric acid—New aspects and challenges. *Electrochim. Acta* **2004,** *49*, 1233-1247.

(23) Garcia-Araez, N.; Rodriguez, P.; Navarro, V.; Bakker, H. J.; Koper, M. T. Structural effects on water adsorption on gold electrodes. *J. Phys. Chem. C* **2011,** *115*, 21249-21257.

(24) Garcia-Araez, N.; Rodriguez, P.; Bakker, H. J.; Koper, M. T. Effect of the surface structure of gold electrodes on the coadsorption of water and anions. *J. Phys. Chem. C* **2012,** *116*, 4786-4792.

(25) Miyake, H.; Hosono, E.; Osawa, M.; Okada, T. Surface-enhanced infrared absorption spectroscopy using chemically deposited Pd thin film electrodes. *Chem. Phys. Lett.* **2006,** *428*, 451-456.

(26) Pronkin, S.; Wandlowski, T. ATR-SEIRAS—an approach to probe the reactivity of Pd-modified quasi-single crystal gold film electrodes. *Surf. Sci.* **2004,** *573*, 109-127.

(27) Miyake, H.; Ye, S.; Osawa, M. Electroless deposition of gold thin films on silicon for surface-enhanced infrared spectroelectrochemistry. *Electrochem. Commun.* **2002,** *4*, 973-977.

(28) Yan, Y.-G.; Li, Q.-X.; Huo, S.-J.; Ma, M.; Cai, W.-B.; Osawa, M. Ubiquitous strategy for probing ATR surface-enhanced infrared absorption at platinum group metal− electrolyte interfaces. *J. Phys. Chem. B* **2005,** *109*, 7900-7906.

(29) Huo, S.-J.; Xue, X.-K.; Yan, Y.-G.; Li, Q.-X.; Ma, M.; Cai, W.-B.; Xu, Q.-J.; Osawa, M. Extending in situ attenuated-total-reflection surface-enhanced infrared absorption spectroscopy to Ni electrodes. *J. Phys. Chem. B* **2006,** *110*, 4162-4169.

(30) Brankovic, S.; Wang, J.; Adžić, R. Metal monolayer deposition by replacement of metal adlayers on electrode surfaces. *Surf. Sci.* **2001,** *474*, L173-L179.

(31) McBride, J. R.; Hass, K. C.; Weber, W. H. Resonance-Raman and lattice-dynamics studies of single-crystal PdO. *Phys. Rev. B* **1991,** *44*, 5016-5028.

(32) Zhang, H.; Wang, C.; Sun, H. L.; Fu, G.; Chen, S.; Zhang, Y. J.; Chen, B. H.; Anema, J. R.; Yang, Z. L.; Li, J. F.; Tian, Z. Q. In situ dynamic tracking of heterogeneous nanocatalytic processes by shell-isolated nanoparticle-enhanced Raman spectroscopy. *Nat. Commun.* **2017,** *8*.

(33) El-Aziz, A.; Kibler, L.; Kolb, D. The potentials of zero charge of Pd (1 1 1) and thin Pd overlayers on Au (1 1 1). *Electrochem. Commun.* **2002,** *4*, 535-539.

(34) Alvarez, B.; Climent, V.; Feliu, J.; Aldaz, A. Determination of different local potentials of zero charge of a Pd–Au (111) heterogeneous surface. *Electrochem. Commun.* **2000,** *2*, 427-430.

(35) Surewicz, W. K.; Mantsch, H. H. New insight into protein secondary structure from resolution-enhanced infrared spectra. *Biochim. Biophys. Acta* **1988,** *952*, 115-130.

(36) Pieniazek, P.; Tainter, C.; Skinner, J. Interpretation of the water surface vibrational sum-frequency spectrum. *J. Chem. Phys.* **2011,** *135*, 044701.

(37) Disalvo, E. A.; Frias, M. Water state and carbonyl distribution populations in confined regions of lipid bilayers observed by FTIR spectroscopy. *Langmuir* **2013,** *29*, 6969-6974.

(38) Grossutti, M.; Dutcher, J. R. Correlation between chain architecture and hydration water structure in polysaccharides. *Biomacromolecules* **2016,** *17*, 1198-1204.

(39) Nojima, Y.; Suzuki, Y.; Yamaguchi, S. Weakly hydrogen-bonded water inside charged lipid monolayer observed with heterodyne-detected vibrational sum frequency generation spectroscopy. *J. Phys. Chem. C* **2017,** *121*, 2173-2180.

(40) Su, Z.; Juhaniewicz-Debinska, J.; Sek, S.; Lipkowski, J. Water structure in the sub-membrane region of a floating lipid bilayer-the effect of an ion-channel formation and the channel blocker. *Langmuir* **2020,** *36*, 409-418.

(41) Falk, M. The frequency of the H-O-H bending fundamental in solids and liquids. *Spectrochim. Acta A* **1984,** *40*, 43-48.

(42) Binder, H. Water near lipid membranes as seen by infrared spectroscopy. *Eur. Biophys. J.* **2007,** *36*, 265-279.

(43) Wagner, F. T.; Moylan, T. E. Hydrogen chloride adsorption and coadsorption with hydrogen or water on platinum (111). *Surf. Sci.* **1989,** *216*, 361-385.

(44) Chen, N.; Blowers, P.; Masel, R. Formation of hydronium and water–hydronium complexes during coadsorption of hydrogen and water on (2× 1) Pt (110). *Surf. Sci.* **1999,** *419*, 150-157.

TOC graphic

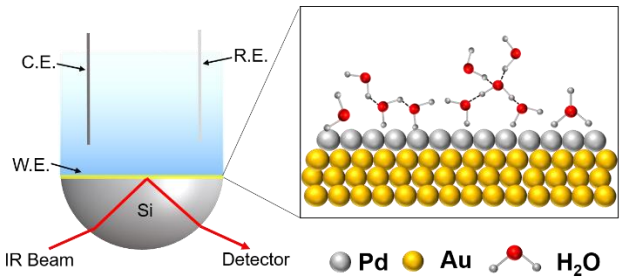
C.E.
R.E.
W.E.
Si
IR Beam
Detector
Pd
Au
H_2O